Atmospheric Environment 47 (2012) 330–340

Contents lists available at SciVerse ScienceDirect

Atmospheric Environment

journal homepage: www.elsevier.com/locate/atmosenv

Urban air quality modeling with full O_3–NO_x–VOC chemistry: Implications for O_3 and PM air quality in a street canyon

Minjoong J. Kim [a], Rokjin J. Park [a,*], Jae-Jin Kim [b]

[a] Atmospheric Chemistry Modeling Laboratory, School of Earth and Environmental Sciences, Seoul National University, Seoul 151-747, Republic of Korea
[b] Department of Environmental Atmospheric Sciences, Pukyong National University, Busan 608-737, Republic of Korea

ARTICLE INFO

Article history:
Received 7 July 2011
Received in revised form
21 October 2011
Accepted 27 October 2011

Keywords:
Street canyon
Urban pollution
Air quality
CFD

ABSTRACT

We examine transport and chemical transformation of reactive pollutants on an urban street using a computation fluid dynamics (CFD) model coupled with full photochemistry of reactive pollutants. An extensive comparison between simulated results and observations is conducted to evaluate the model, focusing on a field campaign occurred in Dongfeng Middle Street in Guangzhou, China. Observed CO and NO concentrations vary diurnally following traffic volumes. The model captures this observed diurnal variation and magnitudes of CO concentrations successfully. However, simulated NO concentration is three times higher than observation. This high bias is significantly reduced in the sensitivity simulation with lower NO_x emissions. We find that oxidation products of O_3 photochemistry such as NO_2 and O_3 vary differently from primary pollutants, indicating important effects of photochemical reactions on their fates. The model appears to reproduce observed O_3 and NO_2 variability with time and altitude. Our analysis shows that high NO_x concentrations in the urban street canyon may efficiently produce aerosol nitrate in the presence of NH_3. Simulated inorganic NO_3^- aerosol concentration reaches up to 0.3 $\mu g\ m^{-3}$ in July but increases an order of magnitude higher at lower temperature that favors partitioning of gas-phase HNO_3 to aerosol-phase, implying a serious concern for urban air quality in winter.

1. Introduction

Previous studies of urban air quality modeling of street canyons have employed high spatial and temporal resolutions of computation fluid dynamical models (CFDs) (Cai et al., 2008). Because of the complexity of dynamical processes depending on the canyon geometry (Hunter et al., 1992; Kim and Baik, 2004; Tsai et al., 2005), most CFD modeling works have focused on dynamical processes and their effects on passive tracers transport and mixing in street canyons (Jeong and Andrews, 2002; Kim and Baik, 2004; Liu and Barth, 2002; Tsai et al., 2005; Vardoulakis et al., 2003). However, primary pollutants emitted from road traffics in urban streets include reactive species such as nitrogen oxides ($NO_x = NO + NO_2$) and volatile organic compounds (VOCs). These species chemically react each other in the presence of sunlight, resultantly producing toxic secondary pollutants such as O_3 and aerosols, which are major concerns for urban air quality (Weschler, 2006).

In order to account for chemical transformation and production of reactive species in the urban street canyon, Baker et al. (2004) first introduced the steady state O_3–NO–NO_2 photochemistry in a large-eddy simulation and showed dissimilar chemical characteristics above and within the street canyon. Since then, a few studies have focused on the turbulent dispersion of reactive pollutants in the street canyon using the steady state O_3–NO–NO_2 photochemistry (Baik et al., 2007; Grawe et al., 2007; Kang et al., 2008). The chemical mechanism used in those studies, however, is too simple to realistically simulate complex chemical processes in urban streets that in particular it excludes important O_3 precursors such as reactive VOCs.

Recently, Liu and Leung (2008) simulated the dispersion of reactive pollutants considering the complex photochemical reactions with VOCs. They found that the high level of O_3, on the order of 100 ppbv and higher, would occur inside the street canyons when considering VOCs emissions. On the other hand, Garmory et al. (2009) have compared results with the steady state O_3–NO–NO_2 photochemistry used in Baker et al. (2004) and with the more complex CBM-IV chemical mechanism with 28 species, and studied the turbulence effect on chemical reactions using stochastic fields. They found no significant differences in NO, NO_2, and O_3 concentrations between the steady state and the CBM-IV cases. We here however argue that the steady state O_3 chemistry

---

[*] Corresponding author. Tel.: +82 2 880 6715.
E-mail address: rjpark@snu.ac.kr (R.J. Park).

1352-2310/$ – see front matter © 2011 Elsevier Ltd. All rights reserved.
doi:10.1016/j.atmosenv.2011.10.059

is too simple to realistically simulate secondary pollutants on an urban street. An accurate assessment of photochemical effects on secondary pollutants such as O_3 is our main objective in this paper.

Urban chemistry is very sensitive to photolysis reactions and thus the use of accurate photolysis rates is important in air quality models (Carter, 1994). Most previous CFD modeling studies have used fixed photolysis rates on a reference time and have not accounted for the diurnal variation. In this study, we coupled a CFD model with a detailed NO_x–O_x–VOCs chemical mechanism and an online photolysis rate computation module to account for the effects of diurnal variation of solar radiation on reactive species concentrations. We use this coupled photochemistry-CFD model to examine the effects of full chemical reactions on reactive pollutant concentrations and their distributions on urban street canyons.

In addition, fine particulate matters (PM) are important issues for urban air quality, affecting human health (Davidson et al., 2005), and large fractions of fine PM are produced by the chemical oxidation of gas-phase precursors such as sulfur dioxide (SO_2) and NO_x and the subsequent gas-to-particle conversion. There are growing interests in understanding PM productions and spatial distributions on urban street canyons (Gidhagen et al., 2005; Kumar et al., 2008a,b). However, chemical reactions have not been considered in previous CFD models for PM studies. We also use our model to simulate PM concentrations on urban street canyons and show possible important PM species for urban air quality.

Several model simulations were conducted to investigate the model sensitivity. In particular, we compare the results from the full chemistry simulation with results from the model using a steady state of NO–NO_2–O_3 photochemistry to show the importance of considering full chemical reactions for accurately simulating secondary pollutants. We also apply the coupled chemistry-CFD model to a case study and evaluate the model by comparing against observations. Finally, factors affecting reactive species concentrations and distribution in an urban street are discussed.

2. Model description

2.1. General description

The numerical model employed in this study is a CFD model based upon the Reynolds-averaged Navier–Stokes equations (RANS) model (Kim and Baik, 2004). The model employs a three dimensional, nonhydrostatic, nonrotating, and incompressible airflow system. It contains a renormalization group (RNG) k–ε turbulence scheme proposed by Yakhot et al. (1992). This scheme differs from the standard k–ε turbulence scheme in that it includes an additional sink term in the turbulence dissipation equation to account for nonequilibrium strain rates and employs different values for the model coefficients (Tutar and Oguz, 2002). The model solves advection equations (Patankar, 1980) using the finite volume method for scalar pollutants. This model was previously used to examine flow and dispersion of scalar pollutants (Kim and Baik, 2004). Furthermore, it has been extended to include reactions and transport of chemical species of NO, NO_2, and O_3 with the steady state photochemistry (Baik et al., 2007; Kang et al., 2008). The model includes updated the boundary conditions for solid bodies in the momentum and thermodynamic energy equations (Kim and Baik, 2010) that properly represent the effects of the wall boundaries with wall functions.

In order to simulate chemical transformation and production of reactive species in the CFD model, we first implement a full tropospheric NO_x–O_x–VOCs chemical mechanism from a global 3-D chemical transport model (GEOS-Chem) developed at the Harvard University modeling group (Bey et al., 2001). The chemical scheme includes 110 species and 343 reactions among which 50 reactions are photochemical reactions. Reaction coefficients have been updated with the recent experimental data from Hermans et al. (2005), Jiménez et al. (2005) and Stark et al. (2008). The chemical computation is done using a gear type solver, Sparse Matrix Vectorized Gear Code (SMVGEAR) (Jacobson and Turco, 1994) that has been widely used in global and regional chemical models. The SMVGEAR is an accurate and efficient solver applicable to a wide variety of multidimensional atmospheric photochemical problems. Among 110 species simulated in the chemistry module, the CFD model transports 28 chemical tracers with chemical lifetimes longer than the transport time step of 0.5 s.

Photolysis rate coefficients are calculated using the Fast-J algorithm of Wild et al. (2000). The FAST-J algorithm was designed to be sufficiently computationally efficient to permit its use in three-dimensional chemical transport models without a significant loss of accuracy. The algorithm accounts for solar extinction by O_3 and aerosols. Monthly total O_3 climatology from satellite observations as a function of latitude, altitude, and time of year is used in the photolysis rate computation (Liu et al., 2006). Mie scattering by aerosols needs to be interactively accounted for the photolysis rates computation (Liu et al., 2006) but is not currently included in the model because the model does not presently simulate all aerosol types. Recently, the Fast-J algorithm has been updated to incorporate missing direct fluxes on lower boundary for the photolysis rate computation and we used the updated version of the Fast-J in our model.

We also consider the shade effect on photolysis rate computation in the model. Especially for the case where the street canyon is laid on east–west direction, the building can make shadow inside of the street canyon during afternoon and affect photolysis rates. We account for the shade effect on photolysis rates following the approach from Koepke et al. (2010) based on differences between the elevation angle of building and the solar elevation angle at each grid point and time step. In addition, the shade within the canyon can affect the sensible and latent heat fluxes at the surface. However, the inclusion of this effect is beyond the scope of our paper and is not considered in this study.

Deposition processes are important to determine the loss of chemical species (Carmichael et al., 1986) and are divided into dry and wet depositions. Currently, our CFD model does not have an atmospheric physics module to simulate hydrometeors such as clouds and rains and thus we do not calculate wet deposition. The dry deposition process is important to calculate night time O_3 concentration (Wesely and Hicks, 2000). We include the dry deposition process following Brasseur et al. (1998).

The exchange of tracers between the street and the urban boundary layer above by the entrainment/detrainment mechanism is important (Patton et al., 2001; Vilà-Guerau de Arellano et al., 2011). However, the model does not explicitly include this mechanism yet. Instead we use the computed profiles of the entrainment/detrainment rates from the previous studies. The O_3 entrainment rate of 2.0×10^5 molecule $cm^{-3}\,s^{-1}$ into top boundary from Ayers et al. (1997) is used. For NO, Vilà-Guerau de Arellano et al. (2011) studied the effect of entrainment/detrainment effect that primarily resulted in dilution of NO from canyons. We employed the calculated NO dilution rates from Ayers et al. (1997) to decrease NO concentrations. The maximum decrease due to mixing with the urban boundary is up to 2%.

Finally, inorganic aerosol species including NH_4^+, NO_3^-, and SO_4^{2-} are computed in the model. Sulfate aerosol is produced mainly from the gas-phase oxidation of SO_2 but aqueous oxidation of SO_2 by H_2O_2 and O_3 in clouds is not considered yet. Other inorganic species of NH_4^+ and NO_3^- are determined in an offline fashion using aerosol thermodynamic equilibrium module, ISORROPIA-II (Fountoukis and Nenes, 2007).

2.2. Simulation setup for case studies

We conducted several simulations for two case studies. One was with the steady state photochemistry reactions of O_3–NO–NO_2 and the other was with the full chemistry scheme discussed above. Fig. 1(a) shows the simulation domain of the steady state O_3–NO–NO_2 photochemistry case that is consistent with that of Baker et al. (2004). The building structure is assumed infinitely long and wind direction is perpendicular to the street canyon. The simulated domain size is 24 m × 40 m × 94 m and grid points are 82, 42, and 92 in the x-, y-, and z- direction. The street canyon is located in the middle of x-direction and the canyon width (W) is 18 m. Building heights (H) and widths (B) are 18 m and 6 m, respectively. Thus, the canyon aspect ratio, H/W, is one. The grid intervals in the x- and y-direction are uniform with $\Delta x = 0.3$ m and $\Delta y = 1$ m and the grid size in the z-direction is uniform up to grid number 61 with $\Delta z = 0.3$ m and then increases with an expansion ratio of 1.15. We use area source emissions that cover 30 grid cells placed in the bottom of the street canyon. Emission rates are 1000/30 and 100/30 ppb s^{-1} per each grid for NO and NO_2. The initial O_3 concentration is assumed to be 20 ppbv, following the method in Baker et al. (2004).

Another case is an observed case for reactive tracers with the full chemistry mechanism. In order to evaluate the model, we compare the observed versus simulated reactive species concentrations in section 3. The case chosen here is a field campaign in Guangzhou, China by Xie et al. (2003), who conducted extensive measurements of chemical species and meteorological conditions in Dongfeng Middle Street for July and October, 1999. Observed chemical species include hourly concentrations of CO, NO, NO_2, and O_3 whose vertical profiles within the street canyon were monitored at the southern side of the street by a continuous 24-h automatic monitoring system (Xie et al., 2003). CO concentrations in surface air were also measured hourly using an infrared CO analyzer at 6 different monitoring sites located in both sides of the street.

The street is approximately 32 m wide and has several buildings with heights of 28 ~ 35 m. The aspect ratio of canyon geometry is 0.9 ~ 1.1. The observed prevailing wind directions above the root top varied almost opposite from July to October and were across the street (Xie et al., 2003). As a result, the profile measurements were made at the leeward side in July but at the windward side in October. We mainly focus our analysis on the model results accordingly.

Following the geometry of the street, we devise the model simulation domain as shown in Fig. 1(b). The domain size is 40 m × 238 m × 78 m and the numbers of grid points are 42 × 121 × 62. The sizes of W and B are 30 m and 10 m, respectively. Grid intervals in the x- and y-direction are uniform with $\Delta x = 1$ m and $\Delta y = 2$ m. The grid size in the z-direction is uniform up to grid number 36 with $\Delta z = 1$ m and then increases with an expansion ratio of 1.04. For meteorological conditions, we use observed mean values during the campaign period. The observed daily mean temperatures in the field campaign period were 29 °C and 23.5 °C in July and October, respectively. In order to simulate diurnal changes in buoyance and its effects on the transport and on the chemical reaction rates we use in the model these values with imposed diurnal variation such that maximum temperature occurs at 2 pm with the diurnal temperature range of 10 °C. The surface and the top boundary pressures in the model are assumed to be 1013.15 hPa and 996.68 hPa, respectively.

We estimate primary pollutant emissions from load traffic using traffic volumes measured during the field campaign that were similar for both July and October (Xie et al., 2003). Vehicular NO_x emissions are computed using NO_x emission rates that are different by the vehicle sizes (5.4, 1.1, and 0.1 g km^{-1} for large, medium, and light vehicles and motorcycle, respectively), following the method by Wang et al. (2010). Observed traffic volume of different sized vehicles by Xie et al. (2003) were generally consistent with those by Wang et al. (2010) at Guangzhou in 1999. We then separate NO_x emissions into NO and NO_2 emissions using 10:1 ratio by volume (Buckingham et al., 1997). CO emissions in the model are derived using CO to NO_x ratios, which is 12:1. Total VOCs emissions are estimated using the observed NO_x to VOCs mass ratio of 2.7 from

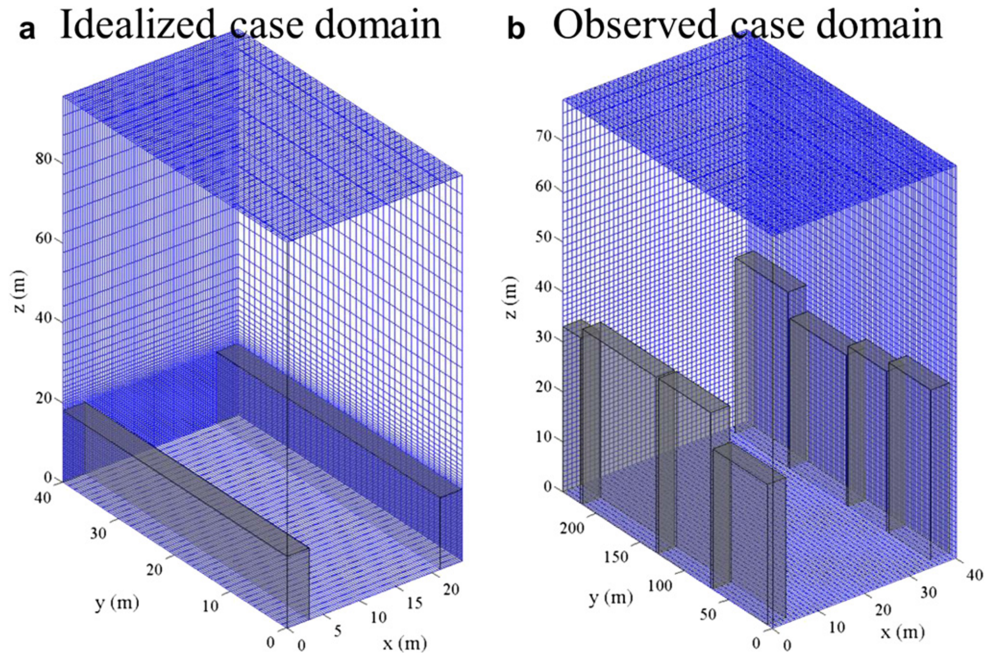

Fig. 1. Schematic diagrams of the coupled chemistry-CFD simulation domains for (a) an idealized case and (b) an observed case, respectively.

Wang et al. (2010) and are speciated further using the method by Kim et al. (2006). The highest emitted VOC is ALK4 (Lumped C4 Alkanes), followed by PRPE (Lumped C3 Alkenes). The estimated ALK4 and PRPE emissions are 27.6 kg day^{-1} and 10.3 kg day^{-1} in the Dongfeng Middle Street. The emissions of ethane, propane, formaldehyde, and acetone are 1242 g day^{-1}, 693 g day^{-1}, 756 g day^{-1}, and 693 g day^{-1}, respectively. The SO_2 and NH_3 emissions of inorganic aerosol precursors in the model are also estimated using respective emissions rates of 56.4 and 61.0 mg km^{-1} per vehicle from Schmid et al. (2001) and Fraser and Cass (1998). Tables 1 and 2 summarize species emissions used in our model simulations.

For the roof top boundary conditions of NO, NO_2, O_3 and CO in the model, we use the observed roof top hourly concentrations that were measured at the leeward side in July (Xie et al., 2003). The observations in October were not used in the model because measurements were conducted at the windward side and were significantly affected by pollution outflow from the inside of the street canyon. We conduct 48 h model simulations for case studies of July and October and the first 24 h is for the model spin-up and the results for the last 24 h are used in our analysis.

3. Model evaluation

3.1. Idealized case with the steady state photochemistry

Baik and Kim (2002) previously evaluated the CFD model used in this study by comparing numerical results with observations from Meroney et al. (1996) and showed that the normalized pollutant concentration in the model was highly correlated with the wind-tunnel measurements with R^2 of 0.86. They also compared the model with wind profiles observations from the water channel facility and showed that the vertical profiles of the normalized wind velocity in the numerical experiment were similar to that in the water channel experiment. Recently, Kim and Baik (2010) implemented the improved wall functions for the momentum and thermodynamic energy equations to represent the effects of the wall boundaries more properly and the model reproduced the vertical profiles of wind and temperature from the wind-tunnel experiment by Uehara et al. (2000) quite well. As discussed above, the CFD model used in this study has been extensively evaluated focusing on dynamics and non-reactive tracer transport (Baik and Kim, 2002; Kim and Baik, 2004, 2010). Therefore, we do not include discussion on the simulated dynamics and the non-reactive tracer transport evaluation but primarily focus on reactive species concentrations.

We evaluate the model with the steady state photochemistry by comparing with the previous model results by Baker et al. (2004) because appropriate observational data are not available for the model validation. Fig. 2 shows NO, NO_2, and O_3 concentrations in ppbv for the comparison with Baker et al.'s results (Fig. 4 in Baker et al., 2004). The simulated NO and NO_2 concentrations at the leeward side are higher than those at the windward side showing a strong vortex feature. The lowest concentrations of NO and NO_2 are shown at the center of vortex and are 195.3 and 34.3 ppbv, respectively. However O_3 is the highest at the center of vortex. These patterns are shown consistently in other modeling studies (Baik et al., 2007; Baker et al., 2004).

Table 1
Emission estimates from vehicles used in the coupled chemistry-CFD model simulations for the campaign by Xie et al. (2003) in Dongfeng Middle Street, Guangzhou, China in July, 1999. Details on the species emission estimates are discussed in the text.

	Moto cycle and light vehicle [kg]	Medium vehicle [kg]	Heavy vehicle [kg]	Total mass [kg]
NO	3.9	4.3	13.9	22.1
NO_2	0.6	0.7	2.1	3.4
CO	46.8	51.6	166.8	265.2
VOC	12.3	13.4	43.2	69.0
SO_2	0.5	0.6	1.8	2.9
NH_4	0.6	0.6	1.9	3.1

Table 2
Same as in Table 1 but for October.

	Moto cycle and light vehicle [kg]	Medium vehicle [kg]	Heavy vehicle [kg]	Total mass [kg]
NO	4.0	4.5	14.4	22.9
NO_2	0.6	0.7	2.2	3.5
CO	47.9	53.8	172.6	274.3
VOC	12.7	13.9	44.7	71.3
SO_2	0.5	0.6	1.8	2.9
NH_4	0.6	0.6	1.9	3.1

However, our simulated NO concentrations show a significant absolute difference up to 100 ppbv from the Baker et al.'s result although its relative error is around 20 ~ 30%. The main reason for this discrepancy is that our study used the CFD model based on the Reynolds-averaged Navier–Stokes equations (RANS) method, whereas Baker et al. (2004) used the large-eddy simulation (LES) method. Gousseau et al. (2011) studied pollutant dispersion differences between RANS and LES methods and showed up to an order of magnitude differences between two methods. In our comparison, the simulated differences of NO and NO_2 concentrations compared to Baker et al. (2004) are around 20 ~ 30% that are relatively small.

3.2. Observed case with the full chemistry in a street canyon

In this section, we apply the coupled chemistry-CFD model to an observed case and compare simulated chemical species concentrations with observations for the model evaluation of reactive species simulations. As far as we are concerned our study is the first attempt to compare the observed versus simulated reactive species concentrations from a CFD model with a full chemistry reaction scheme. By doing this we also examine characteristics of chemically inert versus active species in the street canyon.

Fig. 3 shows simulated and observed CO concentrations in surface air at both sides of the street canyon in July and October. Observed values are hourly concentrations averaged over a month of each campaign period. The concentrations at the leeward side are by factors of 2–3 higher than those at the windward side for both July and October. This CO gradient across the street is driven by the vortex formulated within the street canyon under the condition for which the wind direction at the roof top is perpendicular to the street with wind speed stronger than 2 m s^{-1} (Xie et al., 2003). The CO distribution in the model is consistent with the observed CO by Xie et al. (2003) and with the previous studies (Georgii et al., 1967; Johnson et al., 1972).

Fig. 4 also shows the simulated and observed hourly CO concentrations at different altitudes. Values here are at the leeward side in July and at the windward side in October and other species concentrations elsewhere will be presented this way. The observed CO concentrations peak at around 9 am, decrease in midday, and show another late afternoon peaks at 6 pm, reflecting daily variation of primary emissions from the road traffic. Decreases in CO concentrations during the day are in part due to the oxidation by OH radical. As the altitude increases CO concentration sharply decreases but maintains the similar diurnal variation. These observed features are well captured by the model.

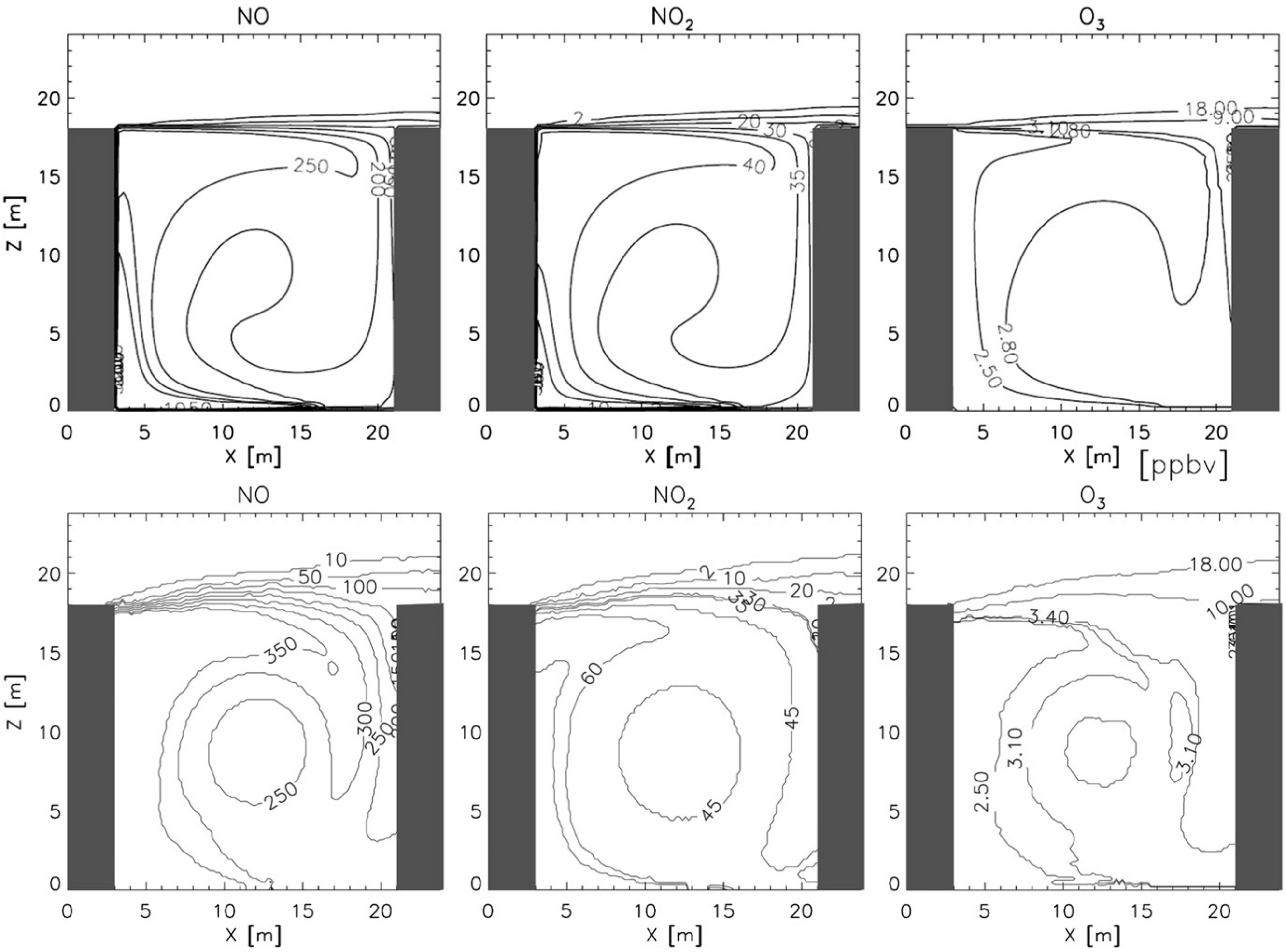

Fig. 2. Comparisons of NO, NO_2 and O_3 concentrations in ppbv using the steady state O_3–NO–NO_2 photochemistry between this work and the previous results by Baker et al. (2004). The values are averaged for the analysis period (75–90 min) and along the street canyon axis. Upper panels are the current modeled results and lower panels are the results by Baker et al. (2004) (Fig. 4 in Baker et al., 2004).

Despite the similar magnitude of CO emissions from the traffic we find that CO concentrations in October observed at the windward side are lower than those in July at the leeward side due to what we discussed above. In typical background air, CO in July is in general lower than that in October due to the efficient chemical loss by OH (Bey et al., 2001) but within the urban street canyon, the dynamical factor appears to be more important. However, one interesting feature is that CO at the roof in October is higher than that in July, reflecting more background characteristics. Xie et al. (2003) explained that higher CO at the windward roof in October was due to the transport from the street canyon by wind vortices. We find that the model successfully captures the observed CO concentrations for both cases. Our analysis of the model results revealed that CO at the leeward roof in July was isolated from the inside of street canyon by strong vortex and was mainly affected by background values, whereas CO at the windward roof in October was affected more significantly from the inside of street canyon by vortex breaking. The good agreement between the model and the observations indicates a successful simulation of dynamic processes and load traffic emissions in the model.

Fig. 5 shows simulated NO concentrations that show similar diurnal variation with CO, indicating a dominant impact of vehicular emissions on NO concentrations. The peaks of NO concentrations occur at 9 am and 6 pm due to high vehicular emissions. After 6 pm the simulated NO concentrations decrease rapidly with time and they are close to zero during the night when NO is quickly converted to NO_2 by O_3 oxidation. We also note a strong vertical gradient of NO concentrations as seen in CO concentrations. Comparing simulated NO with CO, we find also a similar feature such that the higher NO value generally appears in the leeward case but, at the roof, the windward NO is higher than that of the leeward. These characteristics are also generally consistent with the observed NO concentrations that are not shown here but in Xie et al. (2003). However, the simulated values are three times higher than the observations. The difference implies that our simulation may have either insufficient deposition losses or excessive NO emissions in the model. We will discuss the sensitivity of the model to the assumed emissions in section 4.

Simulated NO_2 concentrations are also shown in Fig. 5. They show however a bit different diurnal variations from those of CO and NO. NO_2 concentrations gradually increase with time until late afternoon where peak concentrations occur. There is a slight decrease in midday due to photolysis dissociation of NO_2. Comparing the simulated NO_2 with the observations by Xie et al. (2003), the simulated values are consistent with the observation for both sides. We find however the consistent temporal variation at the windward side of the street canyon in October with the observations but at the leeward side in July observed NO_2 decreased significantly during the daytime inside the canyon that is not captured by the model. During the daytime, NO_2 is formed from

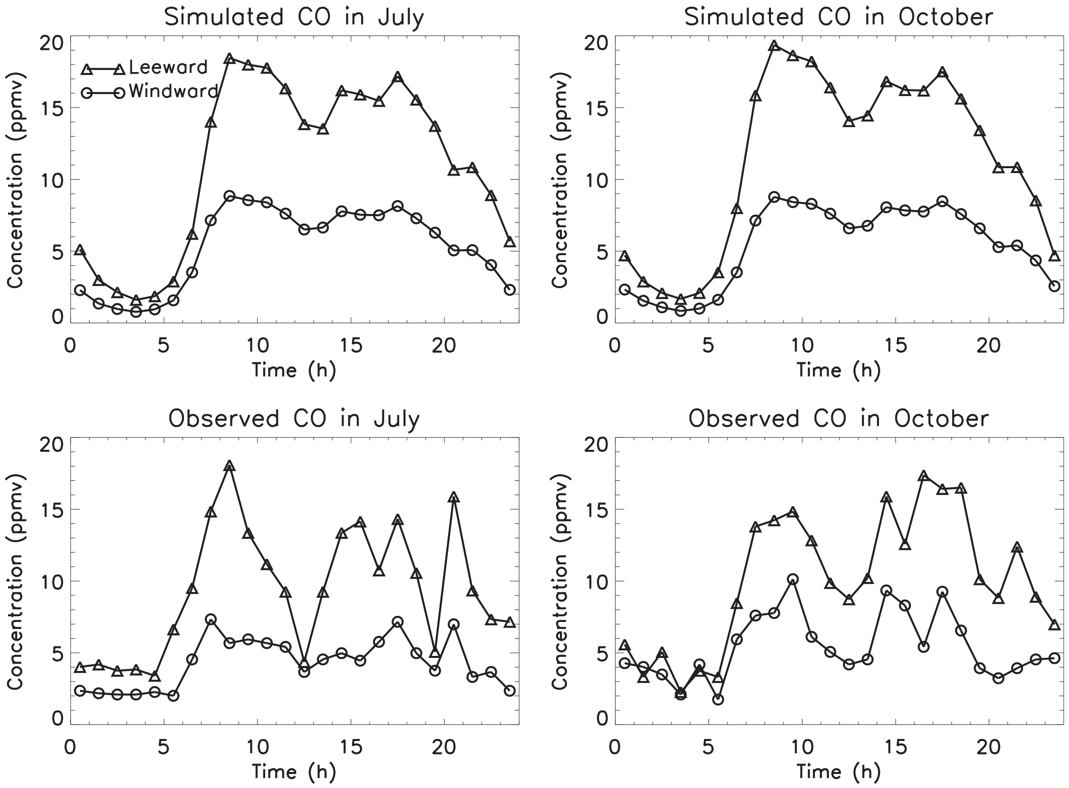

Fig. 3. Simulated (top) and observed (bottom) hourly CO concentrations (ppbv) in Dongfeng Middle Street, Guangzhou, China in July and October, 1999. Observations are from the previous study by Xie et al. (2003). Open triangles and circles indicate values at the leeward side and the windward side of the street canyon, respectively.

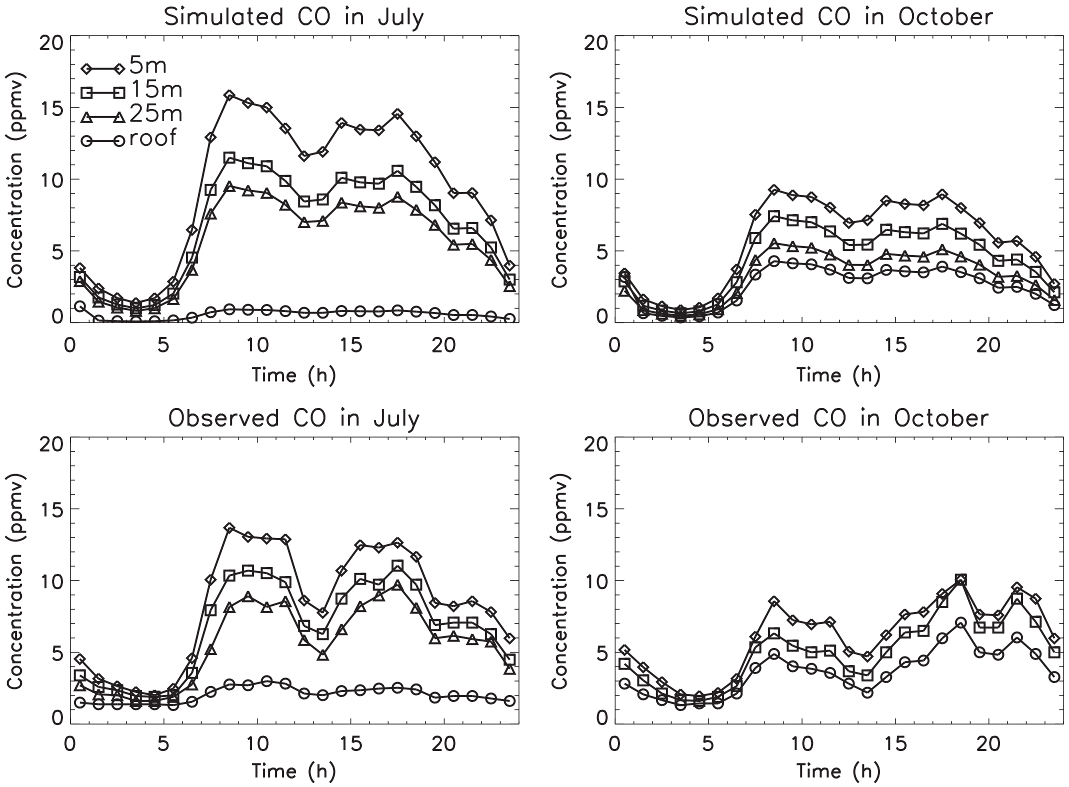

Fig. 4. Simulated (top) and observed (bottom) hourly CO concentrations in ppbv at different altitudes (5 m, 15 m, 25 m, and roof) in Dongfeng Middle Street, Guangzhou, China in July and October, 1999. Observations are from the previous study by Xie et al. (2003). Values in July (left) and October (right) represent concentrations at the leeward side and the windward side of the street canyon, respectively.

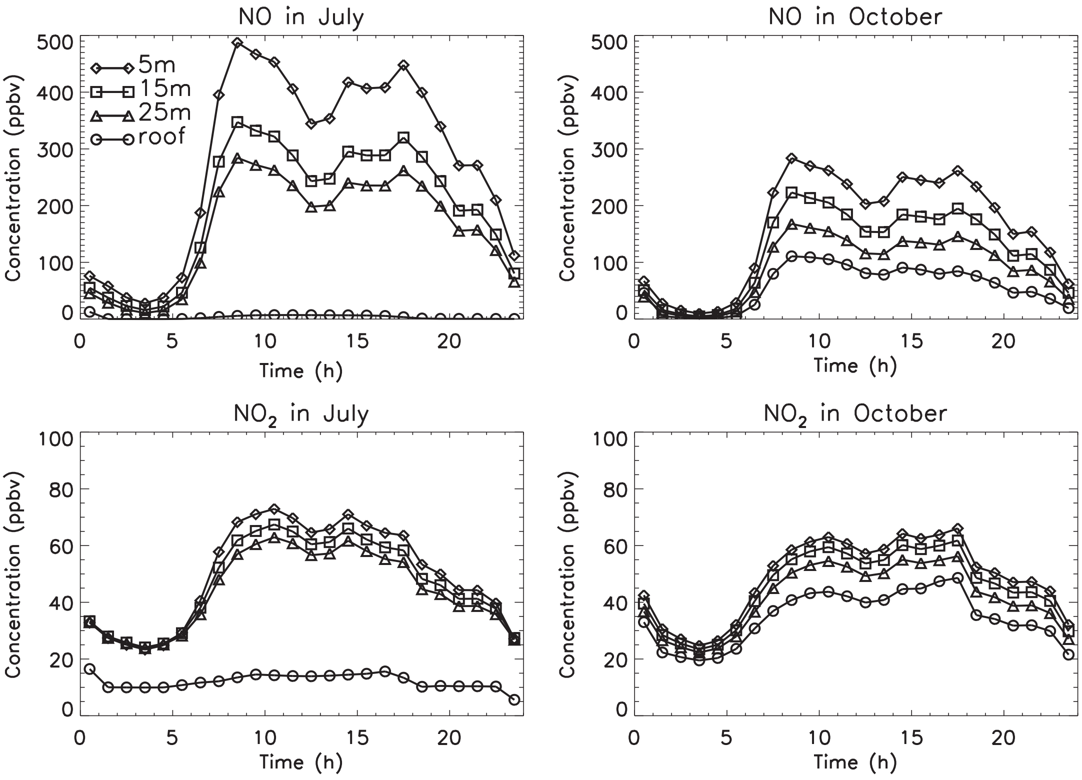

Fig. 5. Same as in Fig. 4 but for simulated hourly NO (top) and NO_2 (bottom) concentrations in ppbv.

the chemical conversion of NO by O_3 or peroxy radicals produced during hydrocarbon oxidations (Jin and Demerjian, 1993). In the presence of sunlight, NO_2 is also quickly dissociated into NO by absorbing solar radiation and produces O_3 (Demerjian et al., 1974). The photo-dissociation of NO_2 could be more dominant in July with stronger insolation, which explains a decrease in observed NO_2 during the daytime in July. In the model, we find that the NO_2 production from NO oxidation is dominant over NO_2 photo-dissociation due to too much NO emission from traffic volume.

Fig. 6 shows simulated O_3 concentrations for July and October. O_3 in urban air is produced by NO_2 photolysis and thus its daily variation follows that of solar zenith angle in general such that peak concentrations occur in mid or early afternoon. Simulated O_3 concentrations show this typical diurnal feature and reach the maximum at 2 pm for both cases. Vertical variation of O_3, however, is dissimilar with those of CO and NO_x such that O_3 concentrations increase with altitude. Despite higher concentrations of O_3 precursor gases within the canyon, O_3 buildup is suppressed by the titration of high NO concentrations due to relatively low VOCs concentrations.

Unlike CO and NO_x, simulated O_3 concentrations at the leeward side in July are lower than those at the windward side in October despite higher precursor concentrations in July (Fig. 5). This is because O_3 production is chemically dependent on the VOCs to NO_x ratio rather than absolute NO_2 concentrations or dynamical transport within the canyon. The simulated VOCs to NO_x ratio at the windward side in October is 1.0, higher than 0.8 at the leeward side in July, indicating the latter case is more severely VOCs limited regime. The simulated ratios do not change significantly throughout the whole day except for early morning when VOCs oxidation by OH leads to a slight decrease in the ratio, which increases again as OH starts oxidizing NO_2 to produce HNO_3.

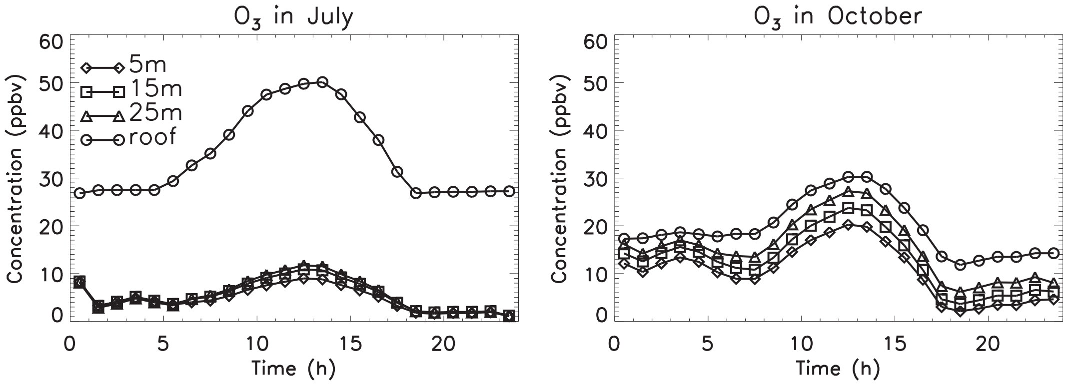

Fig. 6. Same as in Fig. 4 but for simulated hourly O_3.

When we compare the model with the observation by Xie et al. (2003) we find the large discrepancy in July when the observed O_3 concentrations within the canyon did not show any diurnal variations. Xie et al. (2003) suggested the NO_x titration as a main reason for that. However, in October the observed O_3 shows a clear diurnal variation and we do not find any clear explanation for this observed discrepancy.

4. Model sensitivity to chemistry schemes

In order to examine the sensitivity of the model to the full chemistry versus the steady state O_3–NO–NO_2 chemistry we conducted a sensitivity model simulation of the observed case study for July using the latter chemical mechanism. All other conditions are identical. Fig. 7 shows hourly concentrations of NO, NO_2, and O_3 from the sensitivity simulation. Compared with the results with the full chemistry simulation, the concentrations of NO and NO_2 with the steady state chemistry are similar. We find, however, that the simulation with the steady state chemistry results in about 5 ppbv lower O_3 concentrations relative to the full chemistry simulation at 2 pm where the peak concentration occurs. This absolute difference appears to be small because of too low O_3 concentrations due to the strong NO_x titration although the value with the steady state chemistry is two times lower than that of the full chemistry.

We further examine the sensitivities of the model with the chemistry schemes by lowering absolute emissions for less polluted conditions but with the fixed emission ratio of NO_x to VOCs. Table 3 shows maximum O_3 concentrations at 2 pm in the street canyon with different emissions by multiplying the original emission by 0.5, 0.2, and 0.1, respectively. With decreasing emissions the models simulate increasing O_3 concentrations for both chemistry schemes but the factor of 2 relative difference of O_3 between the full chemistry and the steady state chemistry simulations remains consistently. As a result, the absolute difference of O_3 between two schemes increases with decreasing emissions and reaches up to 23 ppbv for the least polluted case. Our sensitivity results imply the importance of the full chemistry simulation for the less polluted urban street.

Garmory et al. (2009) suggested no significant differences in simulated NO, NO_2, and O_3 concentrations between the steady state chemistry and a more complex chemical scheme of CBM-IV cases. However, their study is not consistent with previous chemical transport modeling studies in urban region (Lee et al., 2001; Ran et al., 2011) as well as our results that show a pronounced difference in O_3 concentrations that is mainly due to the VOCs oxidation that expedites O_3 formation through producing HO_2 and other peroxy radicals. These reactive radicals contribute to NO_2 production from the NO oxidation without consuming O_3, resulting in accumulation of O_3 in the canyon.

Table 3
Simulated peak O_3concentrations at 2 pm inside the street canyon for July with different emission rates. The CFD model simulations with the full chemistry are conducted with the estimated and the reduced emissions by factors of 0.5, 0.2, and 0.1, respectively.

Emission rates	Leeward O_3		Windward O_3	
	Steady state chemistry	Full chemistry	Steady state chemistry	Full chemistry
×0.1	10 ppbv	25 ppbv	15 ppbv	38 ppbv
×0.2	9 ppbv	21 ppbv	14 ppbv	36 ppbv
×0.5	7 ppbv	16 ppbv	12 ppbv	26 ppbv
×1.0	5 ppbv	11 ppbv	9 ppbv	24 ppbv

All the model simulations above were conducted based on the estimated vehicular emissions, keeping the fixed VOCs to NO_x emission ratio of one, which is an extremely NO_x rich condition. Considering the large uncertainties of the estimated vehicular emissions depending on ages and driving conditions of vehicles (Frey et al., 2002; Holmén and Niemeier, 1998) we conduct an additional sensitivity run by lowering NO_x emission by half to examine its effect on simulated reactive species concentrations. We keep all other conditions identical and the resulting VOCs to NO_x emission ratio becomes 2.

Fig. 8 shows simulated hourly concentrations of NO, NO_2, and O_3 in July from the sensitivity simulation with the half of NO_x emissions. Compared with the results with original emissions (left panels in Figs. 5 and 6), NO is two times lower, resulting in a much better agreement with the observations. Simulated NO_2 is not much different from the baseline simulation. The most notable change is shown in simulated O_3 that becomes two times higher than the baseline value. This O_3 enhancement is mainly due to relative increases in peroxy radical oxidation of NO and reduces the low bias in the model compared with the observations. However, clear diurnal variation of simulated O_3 concentration is still not consistent with the observation. By lowering estimated NO_x emissions we find that the model generally shows improved agreement with the observations and reveals higher sensitivity of the model with respect to the chemistry scheme. Although there are still some biases in the model that are not fully resolved yet, our results clearly reveal the importance of the full chemistry simulation for air quality modeling of an urban street canyon.

5. Implication for PM air quality in a street canyon

Automobile emissions include not only O_3 precursors such as NO_x, CO, and VOCs, but also SO_2 and NH_3 that are precursors for fine aerosols like sulfate and ammonium. NO_x is also a precursor gas for nitrate aerosol that is produced by the reaction between NH_3 and HNO_3. Fine aerosols are important pollutants for human health and visibility degradation. Simulations of these aerosols with CFD

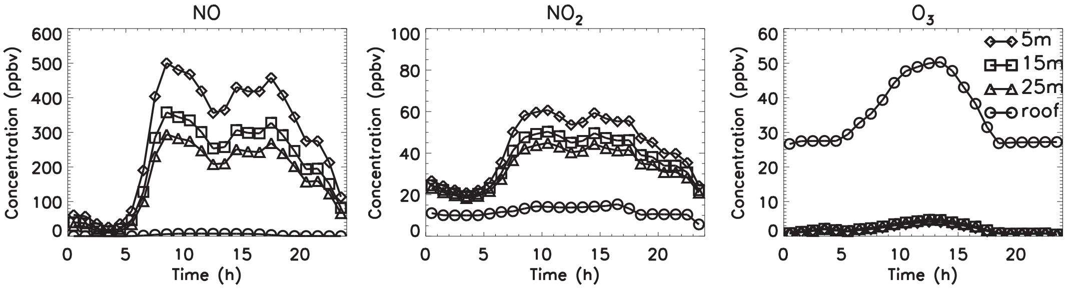

Fig. 7. Same as in Fig. 4 but for simulated hourly NO (left), NO_2 (middle), and O_3 (right) concentrations (ppbv) in July using the steady state chemistry.

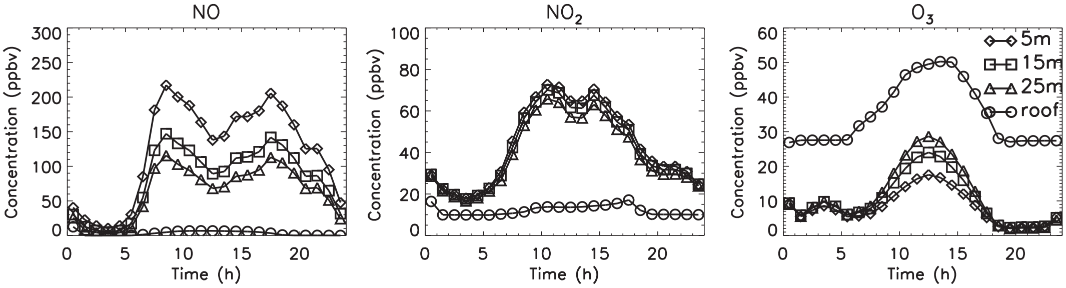

Fig. 8. Same as in Fig. 4 but for simulated hourly NO (left), NO_2 (middle), and O_3 (right) concentrations (ppbv) in July using reduced NO_x emission by half.

models require a consideration of a full chemical mechanism but have not extensively been studied on an urban scale yet. We here also examine simulated secondary aerosols from the model applied to the observed case study above. Inorganic aerosols concentrations including sulfate, ammonium and nitrate are computed in an off-line fashion using the ISORROPIA-II model (Fountoukis and Nenes, 2007; Nenes et al., 1999) such that hourly simulated NH_3, HNO_3, and SO_4^{2-} concentrations from the coupled CFD-chemistry model are provided into the ISORROPIA as input and aerosol thermodynamic computation is performed.

Fig. 9 shows simulated NH_3, $HNO_3$and SO_2 concentrations at the leeward side of the street canyon in July. The peak NH_3 and HNO_3 concentrations are 13.2 and 4.5 ppbv, respectively, and the values are typical found in polluted megacities in China. Since NH_3 does not participate in the gas-phase chemistry in the model its diurnal variation follows that of traffic volumes that are a major source in the urban street, whereas HNO_3 shows a sinusoidal change, peaking at noon when OH concentration is the highest. SO_2 shows similar diurnal variation with CO and amounts up to 5.2 ppbv.

Simulated sulfate aerosol concentration is also shown in Fig. 9 and shows strong diurnal variation following that of OH by which SO_2 oxidation is the major pathway for sulfate production in the model. The highest sulfate aerosol concentration is 0.2 $\mu g\,m^{-3}$ that is relatively low reflecting the minor contribution of SO_2 emission from automobile. Fig. 9 shows calculated nitrate and ammonium aerosol concentrations at the leeward side of the street canyon. Simulated nitrate aerosol has daily variation following its precursor, HNO_3, and its concentration reaches up to 0.3 $\mu g\,m^{-3}$ at noon. Simulated ammonium aerosol concentrations show a similar pattern, indicating its presence as ammonium nitrate. Total inorganic aerosol concentration ($SO_4^{2-} + NH_4^+ + NO_3^-$) simulated in the model is up to 0.7 $\mu g\,m^{-3}$ in the street canyon solely due to the secondary formation from the precursors emitted from the traffic. However this value does not include contributions by other primary aerosols directly emitted and background aerosols produced from other anthropogenic sources that may amount up to higher concentrations.

We find that ammonium nitrate aerosol is the dominant aerosol species in the street canyon based on the model simulation for July. Its formation highly depends on temperature. In order to examine the sensitivity of simulated ammonium nitrate concentrations to the assumed temperature we also conducted another model

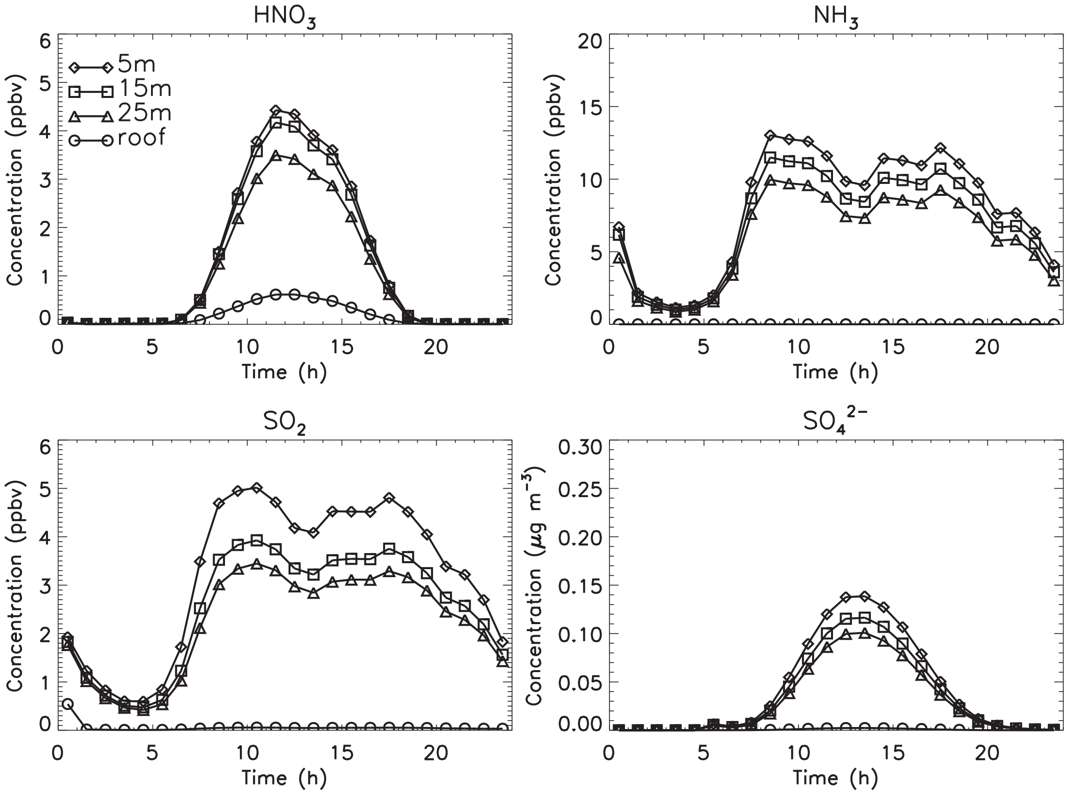

Fig. 9. Simulated hourly HNO_3, NH_3, SO_2 and SO_4^{2-} concentrations in $\mu g\,m^{-3}$ at the leeward side of the street canyon in July.

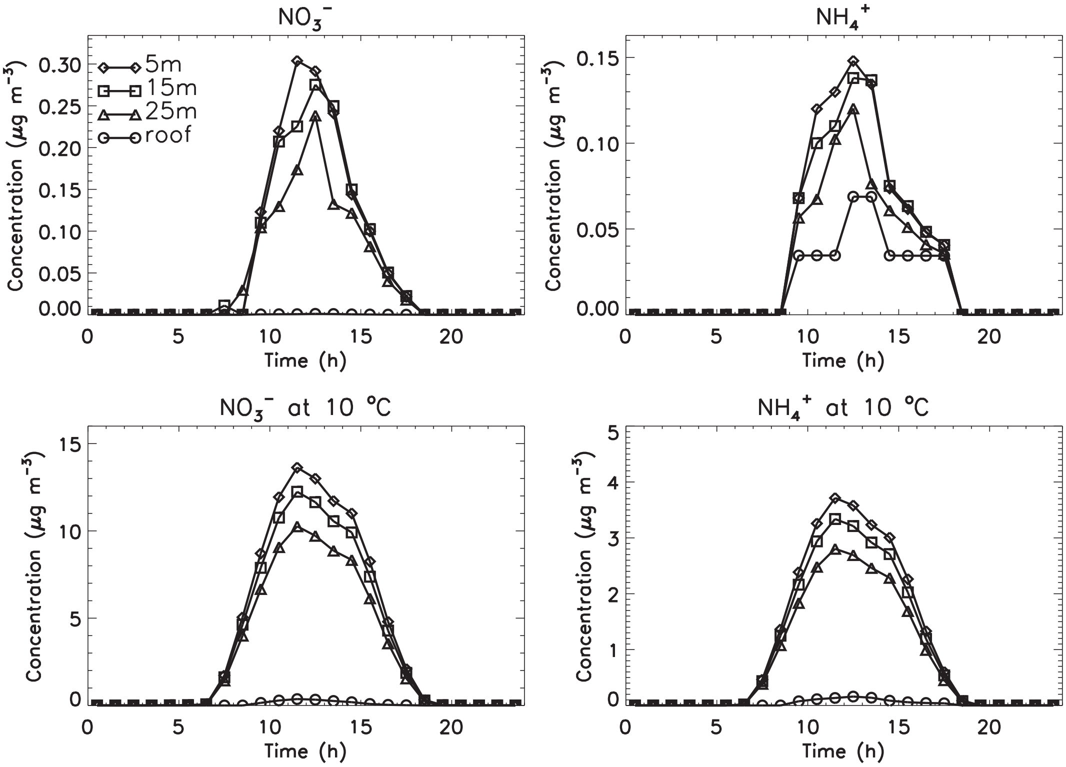

Fig. 10. Simulated hourly NO_3^- and NH_4^+ aerosol concentrations in μg m^{-3} at the leeward side of the street canyon in July. Lower two panels show simulated NO_3^- and NH_4^+ aerosol concentrations in the model using the identical conditions in the top but for 10 °C temperature.

simulation with identical conditions except for 10 °C, a typical mean winter temperature in Guangzhou, China. Fig. 10 also shows ammonium and nitrate aerosol concentrations with 10 °C. The simulated ammonium and nitrate aerosols concentrations are up to 3.7 and 13.6 μg m^{-3}, respectively, that are about an order of magnitude higher than those in July. We found that most HNO_3 partitioned into ammonium nitrate aerosol at low temperature in the presence of NH_3. This result indicates that, inside the street canyon, the PM air quality issue can be more severe in winter than in summer and is mainly due to ammonium nitrate aerosol that is chemically produced by precursor gases from the traffic.

6. Conclusion

Urban air quality modeling on a street canyon is one of the challenging issues because of its complexity. We developed a coupled CFD-chemistry model for simulating air quality on a street canyon considering the full photochemical mechanism. We first evaluated the developed model with the steady state O_3–NO–NO_2 photochemistry by comparing against the previous modeling study. The good agreement with the previous study assured the dynamical and chemical simulations in the model for the idealized case.

We applied the model to the observed campaign occurred in Dongfeng Middle Street, Guangzhou, China in July and October, 1999. We conducted extensive comparisons between the model and the observations by Xie et al. (2003). The simulated CO concentration was in good agreement with the observation, showing a general feature of pollutant dispersion in the street canyon. However, the simulated NO concentration is three times higher than the observation, implying either insufficient depositions or excessive NO emissions in the model. The simulated NO_2 concentrations show a bit different diurnal variations from those of CO due to the photochemical oxidation in the afternoon. O_3 shows a clear sinusoidal variation reflecting its formation solely by the photochemistry. We found also that the photochemical O_3 production within the canyon was suppressed by high NO concentrations in the model. When we compared the model with the observation by Xie et al. (2003) we found the large discrepancy in July when the observed O_3 concentrations within the canyon did not show any diurnal variations.

Our sensitivity simulations with the simple steady state chemistry versus the more complex chemical scheme revealed a considerable difference in O_3 concentrations in the street canyon especially for the less polluted case. By lowering estimated NO_x emissions relative to the baseline simulation the model resulted in improved agreement with the observations and showed higher sensitivity of the model with respect to the chemistry scheme. Although there are still some biases in the model that are not fully resolved yet, our results clearly revealed the importance of the full chemistry simulation for air quality modeling of an urban street canyon.

Finally, we investigated PM air quality inside the street canyon using the model results. NO_x, NH_3, and SO_2 gases emitted from automobiles produced secondary inorganic aerosols. We found that the simulated inorganic aerosol concentrations increased up to 0.7 μg m^{-3} in July. Our sensitivity simulation assuming 10 °C temperature for winter showed that the resulting aerosol concentrations increased up to 17 μg m^{-3} that were about an order of magnitude higher than those in July because most HNO_3 partitioned into ammonium nitrate aerosol at low temperature. This result implied that the PM air quality could be worse in winter inside the street canyon due to the traffic emissions.

Acknowledgements

This study was funded by the Korea Meteorological Administration Research and Development Program under Grant CATER 2007-3205.

References

Ayers, G.P., Granek, H., Boers, R., 1997. Ozone in the marine boundary layer at cape grim: model simulation. Journal of Atmospheric Chemistry 27, 179–195.

Baik, J.J., Kang, Y.S., Kim, J.J., 2007. Modeling reactive pollutant dispersion in an urban street canyon. Atmospheric Environment 41, 934–949.

Baik, J.J., Kim, J.J., 2002. On the escape of pollutants from urban street canyons. Atmospheric Environment 36, 527–536.

Baker, J., Walker, H.L., Cai, X., 2004. A study of the dispersion and transport of reactive pollutants in and above street canyons – a large eddy simulation. Atmospheric Environment 38, 6883–6892.

Bey, I., Jacob, D.J., Yantosca, R.M., Logan, J.A., Field, B.D., Fiore, A.M., Li, Q., Liu, H.Y., Mickley, L.J., Schultz, M.G., 2001. Global modeling of tropospheric chemistry with assimilated meteorology: model description and evaluation. Journal of Geophysical Research D: Atmospheres 106, 23073–23095.

Brasseur, G.P., Hauglustaine, D.A., Walters, S., Rasch, R.J., Müller, J.F., Granier, C., Tie, X.X., 1998. MOZART, a global chemical transport model for ozone and related chemical tracers 1. Model description. Journal of Geophysical Research D 103, 28265–28289.

Buckingham, C., Clewley, L., Hutchinson, D., Sadler, L., Shah, S., 1997. London Atmospheric Emissions Inventory. London Research Centre, London.

Cai, X.M., Barlow, J.F., Belcher, S.E., 2008. Dispersion and transfer of passive scalars in and above street canyons–Large-eddy simulations. Atmospheric Environment 42, 5885–5895.

Carmichael, G.R., Peters, L.K., Kitada, T., 1986. A second generation model for regional-scale transport/chemistry/deposition. Atmospheric Environment – Part A General Topics 20, 173–188.

Carter, W.P.L., 1994. Development of ozone reactivity scales for volatile organic compounds. Journal of the Air and Waste Management Association 44, 881–899.

Davidson, C.I., Phalen, R.F., Solomon, P.A., 2005. Airborne particulate matter and human health: a review. Aerosol Science and Technology 39, 737–749.

Demerjian, K.L., Kerr, J.A., Calvert, J.G., 1974. Mechanism of photochemical smog formation. In: Advances in Environmental Science and Technology, vol. 4. Wiley, New York, pp. 1–262.

Fountoukis, C., Nenes, A., 2007. ISORROPIAII: a computationally efficient thermodynamic equilibrium model for $K^+–Ca^{2+}–Mg^{2+}–NH_4^+–Na^+–SO_4^{2-}–NO_3^-–Cl^-–H_2O$ aerosols. Atmospheric Chemistry and Physics 7, 4639–4659.

Fraser, M.P., Cass, G.R., 1998. Detection of excess ammonia emissions from in-use vehicles and the implications for fine particle control. Environmental Science and Technology 32, 1053–1057.

Frey, H.C., Unal, A., Chen, J., 2002. Recommended strategy for on-board emission data analysis and collection for the new generation model, Prepared for Office of Transportation and Air Quality. US Environmental Protection Agency.

Garmory, A., Kim, I.S., Britter, R.E., Mastorakos, E., 2009. Simulations of the dispersion of reactive pollutants in a street canyon, considering different chemical mechanisms and micromixing. Atmospheric Environment 43, 4670–4680.

Georgii, H.W., Busch, H.W., Weber, E., 1967. Investigation of the temporal and spatial distribution of the emission concentration of carbon monoxide in Frankfurt/Main. Report No. 11 of the Institutes for Meteorology and Geophysics of the University of Frankfurt/Main (available as NAPCA translation 0477).

Gidhagen, L., Johansson, C., Langner, J., Foltescu, V.L., 2005. Urban scale modeling of particle number concentration in Stockholm. Atmospheric Environment 39, 1711–1725.

Grawe, D., Cai, X.M., Harrison, R.M., 2007. Large eddy simulation of shading effects on NO_2 and O_3 concentrations within an idealised street canyon. Atmospheric Environment 41, 7304–7314.

Gousseau, P., Blocken, B., Stathopoulos, T., van Heijst, G.J.F., 2011. CFD simulation of near-field pollutant dispersion on a high-resolution grid: a case study by LES and RANS for a building group in downtown Montreal. Atmospheric Environment 45, 428–438.

Hermans, I., Müller, J.F., Nguyen, T.L., Jacobs, P.A., Peeters, J., 2005. Kinetics of α-hydroxy-alkylperoxyl radicals in oxidation processes. $HO_2^{\bullet}$-initiated oxidation of ketones/aldehydes near the tropopause. The Journal of Physical Chemistry A 109, 4303–4311.

Holmén, B.A., Niemeier, D.A., 1998. Characterizing the effects of driver variability on real-world vehicle emissions. Transportation Research Part D: Transport and Environment 3, 117–128.

Hunter, L.J., Johnson, G.T., Watson, I.D., 1992. An investigation of three-dimensional characteristics of flow regimes within the urban canyon. Atmospheric Environment – Part B Urban Atmosphere 26B, 425–432.

Jacobson, M.Z., Turco, R.P., 1994. SMVGEAR: a sparse-matrix, vectorized Gear code for atmospheric models. Atmospheric Environment 28, 273–284.

Jeong, S.J., Andrews, M.J., 2002. Application of the k-[var epsilon] turbulence model to the high Reynolds number skimming flow field of an urban street canyon. Atmospheric Environment 36, 1137–1145.

Jiménez, E., Gierczak, T., Stark, H., Burkholder, J.B., Ravishankara, A.R., 2005. Quantum yields of OH, HO_2 and NO_3 in the UV photolysis of HO_2NO_2. Physical Chemistry Chemical Physics 7, 342–348.

Jin, S., Demerjian, K., 1993. A photochemical box model for urban air quality study. Atmospheric Environment – Part B Urban Atmosphere 27, 371–387.

Johnson, W.B., Ludwig, F.L., Dabberat, W.F., Allen, R.L., 1972. An urban diffusion simulation model for carbon monoxide. Journal of the Air Pollution Control Association 23, 490–498.

Kang, Y.S., Baik, J.J., Kim, J.J., 2008. Further studies of flow and reactive pollutant dispersion in a street canyon with bottom heating. Atmospheric Environment 42, 4964–4975.

Kim, J.J., Baik, J.J., 2004. A numerical study of the effects of ambient wind direction on flow and dispersion in urban street canyons using the RNG k-[var epsilon] turbulence model. Atmospheric Environment 38, 3039–3048.

Kim, J.J., Baik, J.J., 2010. Effects of street-bottom and building-roof heating on flow in three-dimensional street canyons. Advances in Atmospheric Sciences 27, 513–527.

Kim, M.S., Kim, J.H., Park, H.S., Sun, Y.S., Kim, H.S., Choi, K.H., Yi, J., 2006. Emission inventory of VOCs from mobile sources in a metropolitan region. Korean Journal of Chemical Engineering 23, 919–924.

Koepke, P., Garhammer, M., Hess, M., Roeth, E.P., 2010. NO_2 photolysis frequencies in street canyons. Atmospheric Chemistry and Physics 10, 7457–7466.

Kumar, P., Fennell, P., Britter, R., 2008a. Effect of wind direction and speed on the dispersion of nucleation and accumulation mode particles in an urban street canyon. Science of the Total Environment 402, 82–94.

Kumar, P., Fennell, P., Langley, D., Britter, R., 2008b. Pseudo-simultaneous measurements for the vertical variation of coarse, fine and ultrafine particles in an urban street canyon. Atmospheric Environment 42, 4304–4319.

Lee, S.C., Lam, S., Kin Fai, H., 2001. Characterization of VOCs, ozone, and PM10 emissions from office equipment in an environmental chamber. Building and Environment 36, 837–842.

Liu, C.H., Barth, M.C., 2002. Large-Eddy simulation of flow and scalar transport in a modeled street canyon. Journal of Applied Meteorology 41, 660–673.

Liu, C.H., Leung, D.Y.C., 2008. Numerical study on the ozone formation inside street canyons using a chemistry box model. Journal of Environmental Sciences 20, 832–837.

Liu, H., Crawford, J.H., Pierce, R.B., Norris, P., Platnick, S.E., Chen, G., Logan, J.A., Yantosca, R.M., Evans, M.J., Kittaka, C., Feng, Y., Tie, X., 2006. Radiative effect of clouds on tropospheric chemistry in a global three-dimensional chemical transport model. Journal of Geophysical Research 111, D20303. doi:10.1029/2005JD006403.

Meroney, R.N., Pavageau, M., Rafailidis, S., Schatzmann, M., 1996. Study of line source characteristics for 2-D physical modelling of pollutant dispersion in street canyons. Journal of Wind Engineering and Industrial Aerodynamics 62, 37–56.

Nenes, A., Pandis, S.N., Pilinis, C., 1999. Continued development and testing of a new thermodynamic aerosol module for urban and regional air quality models. Atmospheric Environment 33, 1553–1560.

Patankar, S.V., 1980. Numerical Heat Transfer and Fluid Flow. McGraw-Hill, New York, pp. 126–131.

Patton, E., Davis, K., Barth, M., Sullivan, P., 2001. Decaying scalars emitted by a forest canopy: a numerical study. Boundary-Layer Meteorology 100, 91–129.

Ran, L., Zhao, C.S., Xu, W.Y., Lu, X.Q., Han, M., Lin, W.L., Yan, P., Xu, X.B., Deng, Z.Z., Ma, N., Liu, P.F., Yu, J., Liang, W.D., Chen, L.L., 2011. VOC reactivity and its effect on ozone production during the HaChi summer campaign. Atmospheric Chemistry and Physics 11, 4657–4667.

Schmid, H., Pucher, E., Ellinger, R., Biebl, P., Puxbaum, H., 2001. Decadal reductions of traffic emissions on a transit route in Austria – results of the Tauern tunnel experiment 1997. Atmospheric Environment 35, 3585–3593.

Stark, H., Brown, S.S., Burkholder, J.B., Aldener, M., Riffault, V., Gierczak, T., Ravishankara, A.R., 2008. Overtone dissociation of peroxynitric acid (HO_2NO_2): absorption cross sections and photolysis products. Journal of Physical Chemistry A 112, 9296–9303.

Tsai, M.Y., Chen, K.S., Wu, C.H., 2005. Three-dimensional modeling of air flow and pollutant dispersion in an urban street canyon with thermal effects. Journal of the Air and Waste Management Association 55, 1178–1189.

Tutar, M., Oguz, G., 2002. Large eddy simulation of wind flow around parallel buildings with varying configurations. Fluid Dynamics Research 31, 289–315.

Uehara, K., Murakami, S., Oikawa, S., Wakamatsu, S., 2000. Wind tunnel experiments on how thermal stratification affects flow in and above urban street canyons. Atmospheric Environment 34, 1553–1562.

Vardoulakis, S., Fisher, B.E.A., Pericleous, K., Gonzalez-Flesca, N., 2003. Modelling air quality in street canyons: a review. Atmospheric Environment 37, 155–182.

Vilà-Guerau de Arellano, J., Patton, E.G., Karl, T., van den Dries, K., Barth, M.C., Orlando, J.J., 2011. The role of boundary layer dynamics on the diurnal evolution of isoprene and the hydroxyl radical over tropical forests. Journal of Geophysical Research 116, D07304.

Wang, H., Fu, L., Zhou, Y., Du, X., Ge, W., 2010. Trends in vehicular emissions in China's mega cities from 1995 to 2005. Environmental Pollution 158, 394–400.

Weschler, C.J., 2006. Ozone's impact on public health: contributions from indoor exposures to ozone and products of ozone-initiated chemistry. Environmental Health Perspectives 114, 1489–1496.

Wesely, M.L., Hicks, B.B., 2000. A review of the current status of knowledge on dry deposition. Atmospheric Environment 34, 2261–2282.

Wild, O., Zhu, X., Prather, M.J., 2000. Fast-J: accurate simulation of in- and below-cloud photolysis in tropospheric chemical models. Journal of Atmospheric Chemistry 37, 245–282.

Xie, S., Zhang, Y., Qi, L., Tang, X., 2003. Spatial distribution of traffic-related pollutant concentrations in street canyons. Atmospheric Environment 37, 3213–3224.

Yakhot, V., Orszag, S.A., Thangam, S., Gatski, T.B., Speziale, C.G., 1992. Development of turbulence models for shear flows by a double expansion technique. Physics of Fluids A 4, 1510–1520.